

Supplement of Atmos. Chem. Phys., 18, 13329–13343, 2018
<https://doi.org/10.5194/acp-18-13329-2018-supplement>
© Author(s) 2018. This work is distributed under
the Creative Commons Attribution 4.0 License.



Supplement of

Aerosol-induced changes in the vertical structure of precipitation: a perspective of TRMM precipitation radar

Jianping Guo et al.

Correspondence to: Zhanqing Li (zli@atmos.umd.edu) and Jianping Guo (jpguocams@gmail.com)

The copyright of individual parts of the supplement might differ from the CC BY 4.0 License.

1. Seasonal distribution of the number of localized precipitating events

Figure S1 show the seasonal distribution with regard to the number of localized precipitating events used in the main text. For each rain regime, blue and yellow bars represent clean and polluted conditions, respectively. For the shallow regime, the number of localized events under clean/polluted conditions are 11/7, 9/6, 9/16, and 7/7 for spring, summer, autumn, and winter, respectively. By comparison, for stratiform regime, the numbers are 7/3, 3/5, 5/5, and 4/6, while for convective regime, they become 9/5, 6/8, 7/13, and 8/4, respectively. This indicates there are not dramatic seasonal difference in terms of sampling.

2. Correlation between environmental parameters and PM_{10}

To see whether clouds have any influences on aerosols, correlation analyses between cloud cover and ground-based PM_{10} have been performed over the PRD region. As shown in Figure S2, the correlation between cloud cover from MODIS/Aqua and ground-based PM_{10} over the PRD region is negligible. It could be partly due to the fact that PM_{10} concentration is measured on the ground, which is not affected by the sky conditions at all.

Also, we performed correlation analyses between environmental parameters such as pressure vertical velocity, wind shear, low troposphere stability (LTS), and moisture flux divergence (A), and PM_{10} concentrations. LTS is defined as the differences in potential temperature (θ) between the free troposphere (700 hPa) and the surface (i.e., $LTS = \theta_{700\text{hPa}} - \theta_{1000\text{hPa}}$). The results are shown in Figure S3. It can be seen that no significant correlations can be observed, most likely due to the fact that PM_{10} concentrations are closely linked to emissions rather than to meteorology over the PRD region.

3. Z-R relationship stratified by PM_{10}

Both rain rate and radar reflectivity for three categories of rainfall have been derived, so it is possible to estimate how the Z-R relationship might vary with aerosol content. Figure

S4 describes how the Z-R relationship varies with aerosol content. It is difficult to tell whether the Z-R relationship changes with aerosol. This is likely due to the fact that the Z-R relationship is largely affected by hydrometeor size, meteorological factors, among others, rather than aerosol particles. In addition, the radar reflectivity caused by aerosol particles can be negligible compared with hydrometeors.

4. Uncertainties of aerosol effect on vertical structure of precipitation caused by sampling variation with seasons

To check its potential impact induced by the number of precipitation events by seasons (Figure S1), Figure S5 shows the analyses results in the same way as Figure 5 in the main text, but for summer (June, July, and August), given the dominant precipitation falling over the PRD region in summer. Similar differences of normalized contoured frequency by altitude diagram (Δ NCFAD) pattern as shown in Figure 5 suggest limit seasonal contamination. That is mainly because we focus on localized precipitation only, therefore strictly control on weather patterns are performed and seasonal differences are primarily excluded. Furthermore, the potential influences of different dynamic and thermodynamic conditions during different seasons have been mostly revealed in section 3.4 in the main text.

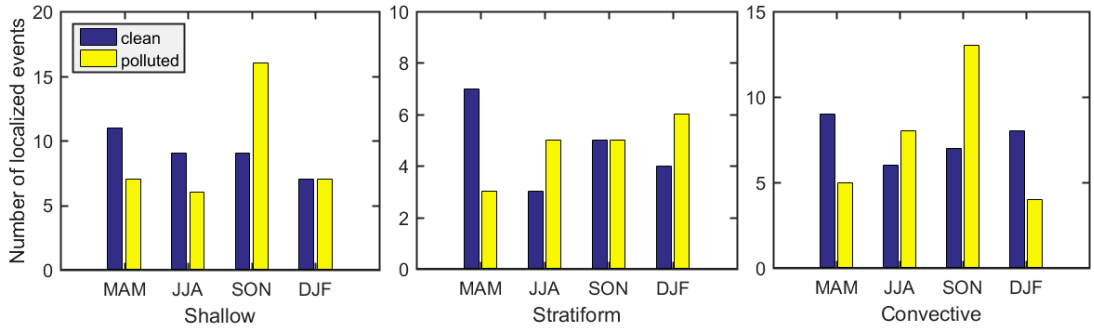


Figure S1. Seasonal distribution of the number of localized precipitating events for spring (March, April, and May), summer (June, July, and August), autumn (September, October, and November), and winter (December, January, and February). For each precipitation regime, blue and yellow bars represent clean and polluted conditions.

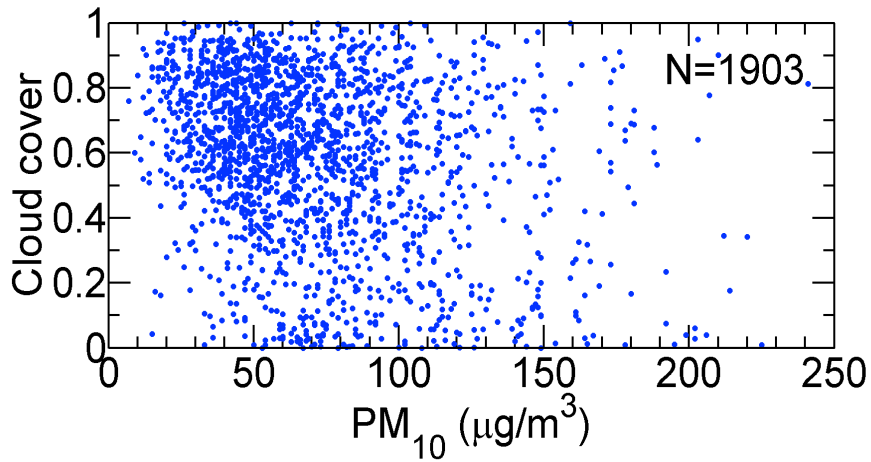


Figure S2. Scatter plot showing the relationship between cloud cover from MODIS/Aqua and ground-based measured PM_{10} over the PRD region. The red line represents the least-squares regression line. The sample size is given by N .

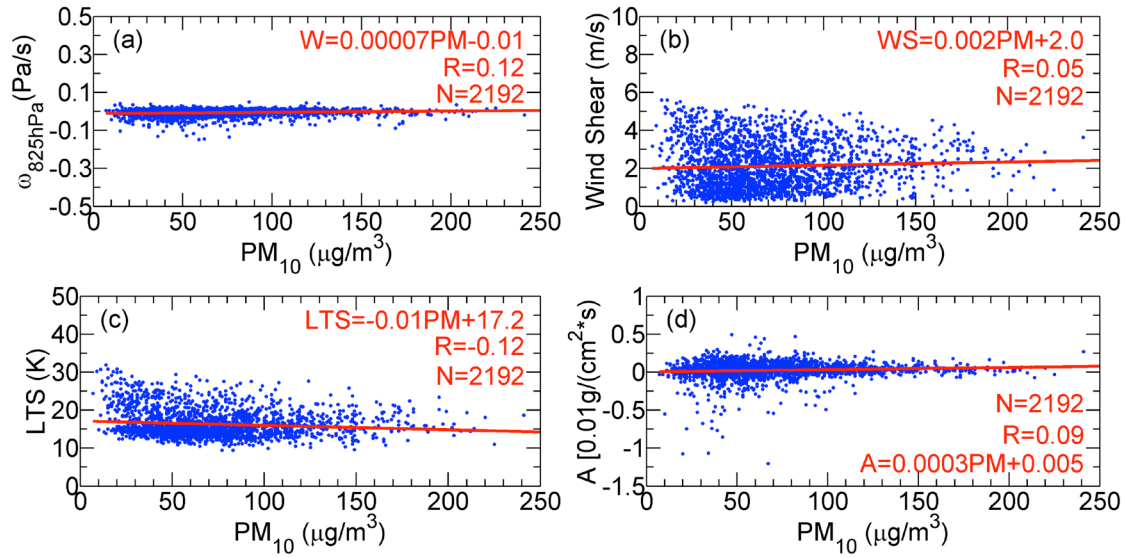


Figure S3. Scatter plots showing the relationships between (a) pressure vertical velocity, (b) vertical wind shear, (c) LTS, and (d) A as a function of ground-based measured PM_{10} over the PRD region. The red lines represent least-squares regression lines.

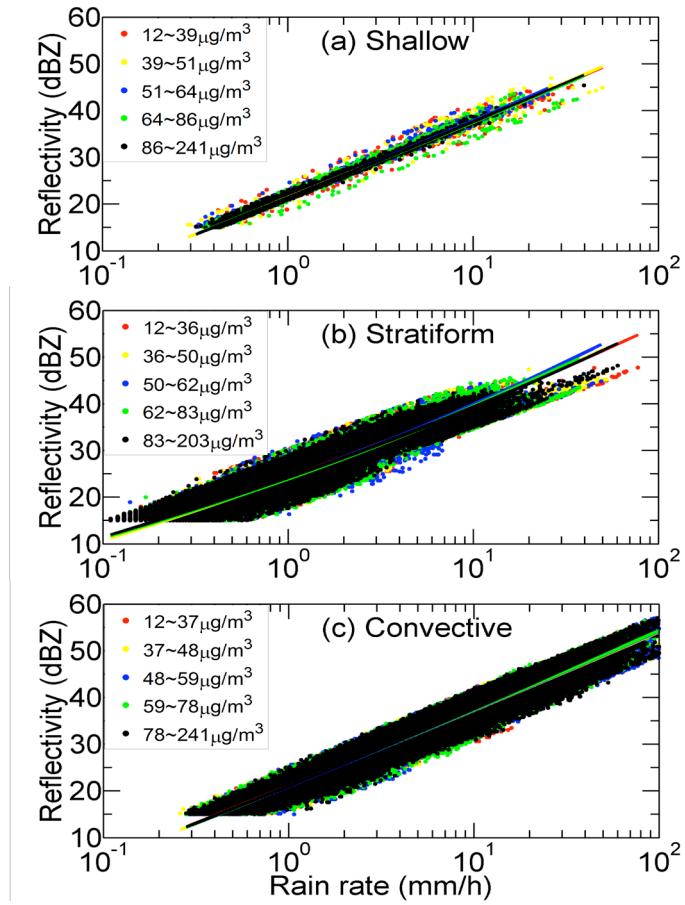


Figure S4. Radar reflectivity as a function of rain rate in different PM₁₀ concentration bins for shallow, stratiform, and convective rain types.

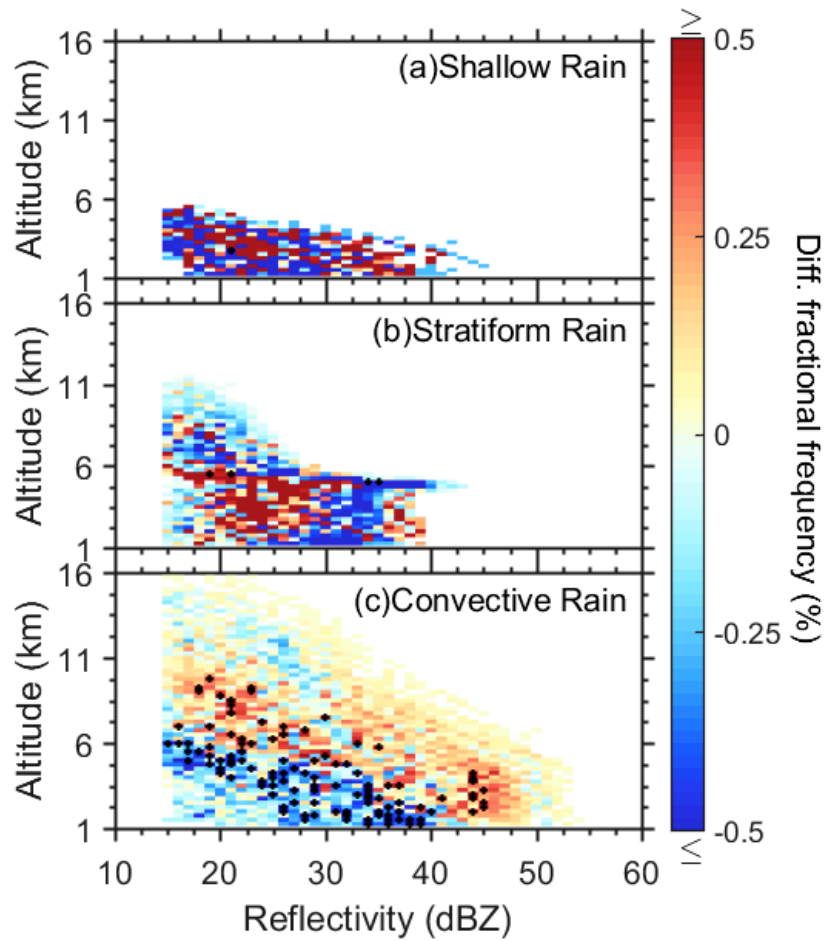


Figure S5. The differences of normalized contoured frequency by altitude diagram (Δ NCFAD) showing the differences in occurrence frequency for detected rain echoes (polluted minus clean) for (a) shallow, (b) stratiform, and (c) convective regimes. Data are from TRMM PR retrievals in summer (June, July, and August), 2007-2012. The black crosses mark grid points where the difference exceeds the 95% significance level ($p < 0.05$) according to the Pearson's χ -square test.